DYNAMIC TEMPERATURE MAPPING OF Nb₃Sn CAVITIES*

R. D. Porter[†], N. Banerjee, M. Liepe

Cornell Laboratory for Accelerator-Based Sciences and Education (CLASSE),
Ithaca, NY 14853, USA

Abstract

Niobium-3 Tin (Nb₃Sn) is the most promising alternative material to niobium for SRF accelerator cavities. The material promises nearly twice the potential accelerating gradients ($\approx 100\,\mathrm{MV/m}$ in TESLA elliptical cavities), increased quality factors, and 4.2 K operation. Current state of the art Nb₃Sn cavities reach quality factors of $2 \cdot 10^{10}$ at 4.2 K and have reached 24 MV/m. Determining the cause of the premature field limitation is the topic of ongoing research. Cornell University has recently developed a high-speed temperature mapping system that can examine cavity quench mechanisms in never before achieved ways. Here we present high-speed temperature map results of Nb₃Sn cavities and examine the quench mechanism and dynamic heating. We show an initial multipacting quench and sudden temperature jumps at multiple locations on the cavity.

INTRODUCTION

Niobium-3 Tin (Nb₃Sn) is the most promising alternative material for superconducting radiofrequency (SRF) accelerator cavities. Nb₃Sn has nearly twice the critical temperature ($T_c = 18\,\mathrm{K}$ vs $T_c = 9.2\,\mathrm{K}$ [1]) and nearly twice the superheating magnetic field ($H_{sh} \approx 425\,\mathrm{mT}$ vs $H_{sh} \approx= 220\,\mathrm{mT}$ [2]) compared to niobium. This allows Nb₃Sn cavities to operate at 4.2 K (where refrigeration is more efficient) at high quality factors $> 2 \cdot 10^{10}$ (at 1.3 GHz) and potentially reach 96 MV/m in TELSA elliptical geometry cavities.

Cornell University has a leading program to create Nb₃Sn accelerator cavities [3–7]. Nb₃Sn is very brittle and must be formed in the final cavity shape. To accomplish this we utilize Sn vapor deposition: a fully formed Nb cavity is placed in an ultra-high vacuum furnace where $SnCl_2$ and Sn is vaporized, allowed to absorb into the surface and forms Nb₃Sn [6, 8]. Additional fabrication techniques such at Chemical Vapor Deposition, Sn-electroplating with thermal conversion, and Nb₃Sn sputtering are being pursued but have not reached the same level of performance [9–15]. After the Sn vapor deposition process our cavities are coated in $2 - 3\,\mu\mathrm{m}$ of Nb₃Sn.

Current Nb₃Sn cavities at Cornell University achieve a quality factor of $2 \cdot 10^{10}$ at 4.2 K and a maximum accelerating gradients of $\approx 17\,\mathrm{MV/m}$ in 1.3 GHz TESLA elliptical cavities. The high quality factor at 4.2 K enables 4.2 K operation and even cryocooler operation [16–18]. The 17 MV/m

maximum accelerating gradient is usable, but far below the theoretical limit. Similar accelerating gradients have been reached at JLab [19] and IMP [20], and recently reached 24 MV/m at FNAL [21]. The cause of premature Nb₃Sn cavity quench is the subject of ongoing research [4, 22, 23].

Temperature mapping has been used to examine quench. Figure 1 shows a quench map of a Nb₃Sn cavity indicating that quench is occurring at a localized spot. This cavity was cut up and the quench site was examined using microscopy, but no obvious quench candidate was observed. Nb₃Sn is sensitive to small defects and temperature maps only have a resolution of $\approx 1\,\mathrm{cm}$ making quench identification difficult.
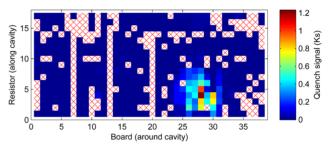

Figure 1: A quench map of a Nb₃Sn cavity taken with the old temperature mapping system [4, 5]. The hot spot in the lower right indicates a localized thermal quench. Quench maps are acquired by allowing the cavity to quench many times and measuring each thermometer in series. Places that are on average hotter are likely the quench site. The plot is displayed as integrated temperature. White squares with red x's indicate non-functional thermometers.

Additional experiments were conducted by D. L. Hall *et al.* where the quench site temperature alone was measured at 25 ksps as the cavity was charged and discharge. The results can be seen in Fig. 2. As the cavity charges we first see Ohmic heating, as expected, but then the temperature suddenly jumps up [5]. When the cavity discharges there are jumps back down, but there is hysteresis between the charge and discharge cycles. The cavity does not quench during the cycle. Furthermore, the jumps appear to be quantized. There has been much speculation as to the cause of the these jumps and how they might be related to quench [4, 23].

These experiments suggest valuable information about the Nb₃Sn quench mechanism could be revealed by time-resolved temperature mapping. The additional information could inform theoretical models of quench or rule out certain quench mechanisms.

Recently, Cornell University has developed a new high-speed temperature mapping system that can resolve the dynamics of RF dissipation [24]. This system samples the entire temperature map 50 ksps, fast enough to resolve cav-
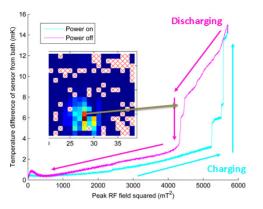
Figure 2: Temperature vs surface magnetic field at the quench site of an Nb_3Sn cavity as the cavity is charged and discharged [4]. Notice the sudden jumps in temperature even though the cavity does not quench.

(a) Picture of the 1.3 GHz temperature map attached to a single cell cavity. Twisted pair ribbon cables have not yet been connected.

(b) Partially removed T-map boards showing location of sensors on the cavity.

Figure 3

ity quench. In addition, this system has very low noise, capable of resolving 15 µK temperature changes in the appropriate configuration (1.8 K with $\approx$ 10000 point averaging at 50 kHz). The high-frequency sampling and low noise could reveal additional dynamics in Nb_3Sn cavities.
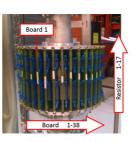
Here we show high-speed/dynamic temperature mapping of Nb_3Sn cavities from Cornell University. These represent preliminary data taken during the commissioning of the temperature mapping system. We find that temperature jumps are widespread, occurring at numerous locations on Nb_3Sn cavities. We find that the first quench appears to be a multipacting quench then quickly moves to a localized spot.

EXPERIMENTAL SETUP

Two Nb_3Sn cavities were tested: LTE1-9 (TESLA geometry) and ERL1-4 (modified TESLA geometry). These cavities received standard Nb_3Sn coatings [8]. Both cavities were tested during the commissioning of the new temperature mapping system. The testing of LTE1-9 was conducted first and some of the data is incomplete or corrupted due to faults in the new system. These faults were fixed before testing ERL1-4. Here we will primarily show data from ERL1-4.

The test system consists of a vertical test pit for testing superconducting RF cavities and a temperature mapping system [24]. Figure 3 shows the T-map on the cavity and a partially removed T-map showing sensor locations. Cernox sensors, fluxgate magnetometers (at top iris), and all standard equipment for RF testing at Cornell is also connected [4]. Due to physical constraints no sensors (other than T-map thermometers) are placed on the cavity equator. Instead, a Cernox sensor is placed near the equator on a T-map board. The T-map data acquisition system is connected to the trigger output of an RF Power Meter to allow simultaneous acquisition of RF and T-map data.

The temperature map consists of 38 boards each with 17 sensors giving 646 thermometers. In addition, 3 sensors are mounted on the boards that do not contact the cavity.

These act as bath sensors. Apiezon N-type grease is used to ensure thermal contact. All thermometers measure a fraction of the cavity wall temperature rise. One estimate finds the thermometers measure 0.35 ± 0.13 of the wall temperature rise. There is further reduced thermal contact with the equator of the cavity due to a rounded weld seam.

The temperature of the bath is subtracted from thermometers in contact with the cavity, giving only the temperature rise of the wall. An RF-off measurement is used to correct for any offsets between the T-map thermometer and the bath sensors.
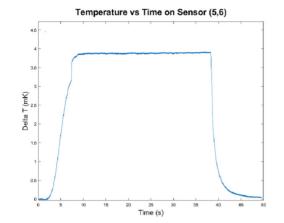
MEASUREMENTS AND DISCUSSION

Temperature Jumps

We can conduct a similar experiment to those conducted by D. L. Hall *et al.* on Nb_3Sn cavities [4, 5]. ERL1-4 was cooled to 1.8 K. The cavity was charged and discharged over a 50 s window while recording the T-map at 25 ksps. The T-map is triggered when the power to the cavity is turned on. We repeated this process many times, gradually raising the forward power—and thus the maximum field in the cavity—until the cavity quenched. The last iteration before quench was conducted at ≈ 0.09 MV/m ± 0.01 MV/m below the quench field.
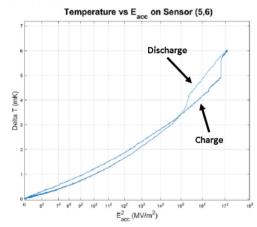
Figure 4 shows one thermometer where temperature jumps were observed. As the cavity is charged a nearly linear (vs the field strength squared) rise in temperature seen then a sudden jump in temperature. As the cavity discharged, we see the opposite (jump down in temperature) but there is a hysteresis. This is similar behavior to that shown by to D. L. Hall *et al.*.

These temperature jumps were observed at many locations on the cavity. Figure 5 marks all thermometers that saw temperature jumps at 1.8 K. There at 59 channels in all. These jumps are of different heights and some channels contain multiple jumps.

Not all temperature jumps are independent: some jumps occur at near-identical timing on adjacent sensors. Thermal

(a) Thermometer temperature versus time during the charge discharge cycle. RF power is turned on at 0 s and the cavity takes ≈ 9 s to charge. The power is turned off at ≈ 40 s and the cavity discharges. A ≈ 0.5 mK temperature jump is observed at ≈ 7 s. A smaller ≈ 0.1 mK jumps is also present but may be difficult to see at this scale.

(b) The same charge-discharge temperature curve but plotted versus the square of the accelerating gradient. In this form the temperature jump during charging is visible, as well as the jump back down.

Figure 4: Temperature jumps observed on one thermometer while the cavity is charged and discharged near the quench field (1.8 K). Some smoothing (1000 point running average) has been applied to make jump features easier to see.
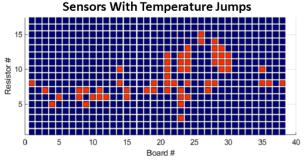

Figure 5: All channels where a temperature jump was observed are marked in red.

SUPCAV003

spread from a single heat source could be warming multiple temperature sensors. We conducted calculations of the thermal distribution of a point heat source in a Nb_3Sn on Nb system. This was done using a version of Cornell's HEAT code [25] modified for multilayer materials. HEAT is a script for solving the equilibrium temperature distribution in SRF cavities and includes BCS resistance, Kapitza resistance, and other temperature dependent phenomena relevant to SRF cavities. Figure 6 shows results (at outer wall) from a thermal simulation of a point heat source (on inner wall) at 2 K and 17 MV/m. At the spacing of our thermometers (≈ 1 cm) the temperature rise drops to ≈ 10% and still measurable by our system. This shows that some adjacent sensors are likely measuring the same temperature jump.
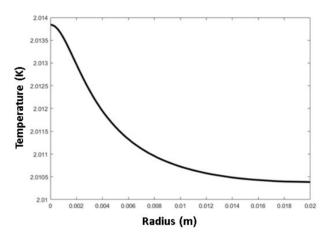

Figure 6: Calculated radial temperature distribution of point thermal defect in a Nb_3Sn cavity as measured from the outer wall. Calculation performed with a bath temperature of 2 K, 8 nΩ of residual surface resistance, and an accelerating gradient of 17 MV/m.

Some thermometers in the temperature map show very little heating (before quench and at 1.8 K). This may be a result of a distribution of residual resistance on the surface or that some sensors have particularly low sensitivity at low temperatures. Low sensitivity sensors may not be able to read temperature jumps below the liquid helium transition point. At 4.2 K, where the helium thermal interface conductance is lower, thermometers read increased heating and additional channels appear to show temperature jumps; however, more measurements and analysis is needed at temperatures above helium transition point to draw a firm conclusion.

Curiously, while D. L. Hall *et al.* observed temperature jumps at the quench site, we did not. This may not indicate a lack of jumps or that jumps are unrelated to quench. One possible explanation is that the first jump to occur was large enough to cause the cavity to quench. Figure 7 shows the distribution of jump heights that were seen in this cavity. Thermal simulations suggest a measured (including approximate thermometer wall sensitivity) temperature jump of 10 − 30 mK would likely cause cavity quench. The largest jump seen so far is 6 mK (see Fig. 1), so this is a plausible explanation.

Figure 7: Histogram of the temperature jump magnitudes seen in ERL1-4.
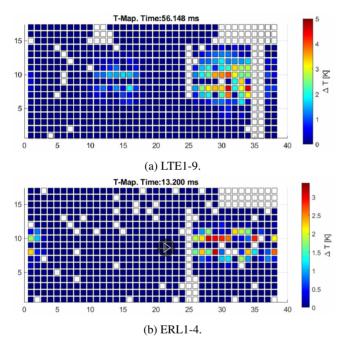

(a) LTE1-9.

(b) ERL1-4.

Figure 8: A frame from a quench T-map video of both LTE1-9 and ERL1-4. These show what appears to be a multipacting quench.

Quench Video

Using the new system, we can record the temperature map as the cavity goes through quench. Figure 8 shows a frame from a T-map video of cavities LTE1-9 and ERL1-4 going through their first quench (after cooldown). Both quenches take place over $\approx 50\,\mathrm{ms}$ and at $17\,\mathrm{MV/m}$. The quench is not localized and is spread preferentially along the equator. The quench did not originate in one spot and spread but turned on across the entire region. This is likely a multipacting quench.

Previous T-maps using non-time-resolved systems showed a different behavior. Figure 1 shows a quench map of a previously measured Nb_3Sn cavity. The quench region is highly

localized and not at the equator. It is not a multipacting quench.

Quench Site Evolution

After the first cavity quench we continued to record the temperature as the cavity went through additional quenches. Figure 9 shows a T-map taken over the next 32 cavity quenches of ERL1-4. We can see that there are now two quench regions: along the equator, and at a localized spot.
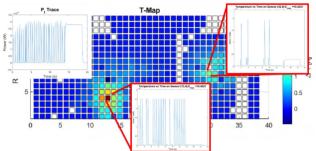

Figure 9: A temperature map showing the average temperature while the cavity is quenched 32 times. Two different hot spots emerge, indicating two quench locations. Two temperature vs time plots are overlayed for a thermometer in each quench region. Large temperature spikes indicate quench at or near the thermometer. Medium height temperature spikes indicate a quench that is still somewhat near (still on the equator). We can see that quench is moving between the equator and the hot spot in the lower left.

Time resolved thermometry reveals that the quenches move back and forth between the two sites. Quenches at the equator show some randomness in location and and relative heating. The second site, however, has highly reproducible dynamics: the same location and relative intensities. After the first 33 quenches the quench site settled on the second, localized site. The next 100 quenches were recorded and all of them occurred at the second site. A possible explanation is that we processed the multipacting site and hit a defect at almost the exact same field, but more study is required.

This also reveals why the multipacting quench was not previously observed. The previous temperature mapping system measure a quench map over 100's of quenches. Since only a handful of the first few quenches are multipacting we could only see the second site in these measurements.

CONCLUSION

Here we have shown the first time-resolved thermometry of niobium-3 tin (Nb_3Sn) SRF cavities. These are only preliminary results, but interesting dynamics are already revealed.

Temperature jumps, previously observed only at the cavity quench site, occur at many places across the cavity surface. Subsequent measurements will hopefully reveal properties that restrict the possible mechanism. We will soon conduct measurements on niobium cavities which will reveal if this phenomenon is part of the Nb_3Sn system or caused by

another aspects of the system (thermometers, helium bath interface, etc.).

Measurements of cavity quench show new dynamics. The first cavity quench appears to be a multipacting quench. The quench site quickly transitions to a second, localized quench site. It is not clear why our Nb_3Sn cavities would be vulnerable to multipacting. Previous measurements found the secondary electron yield of Nb_3Sn is only slightly higher than that of niobium [26]. However, fabrication techniques and processing may impact Nb-Sn ratio, oxides, and adsorb layers which may impact the secondary electron yield. Moving forward both quench mechanisms may need to be investigated to advance Nb_3Sn cavity accelerating gradients.

REFERENCES

[1] A. Godeke, "A Review of the Properties of Nb_3Sn and Their Variation With A15 Composition, Morphology and Strain State," *Superconductor Science and Technology*, vol. 19, no. 8, p. R68, Aug. 2006. `doi:10.1088/0953-2048/19/8/r02`

[2] G. Cetelani and J. P. Sethna, "Temperature Dependence of the Superheating Field for Superconductors in the High-Kappa London Limit," *Phys. Rev. B*, vol. 78, no. 22, p. 224509, Dec. 2008. `doi:10.1103/PhysRevB.78.224509`

[3] S. Posen, "Understanding and Overcoming Limitation Mechanisms in Nb_3Sn Superconducting RF Cavities," Ph.D. dissertation, Phys. Dept., Cornell University, Ithaca, NY, USA, 2014.

[4] D. L. Hall, "New Insights into the Limitations on the Efficiency and Achievable Gradients in Nb_3Sn SRF Cavities," Ph.D. dissertation, Phys. Dept., Cornell University, Ithaca, NY, USA, 2017.

[5] D. L. Hall *et al.*, "Cavity Quench Studies in Nb_3Sn Using Temperature Mapping and Surface Analysis of Cavity Cutouts," in *Proc. SRF'17*, Lanzhou, China, Jul. 2017, paper THPB041.

[6] S. Posen and M. Liepe, "Advances in Development of Nb_3Sn Superconducting Radio-Frequency Cavities," *Phys. Rev. ST Accel. Beams*, vol. 17, p. 112001, Nov. 2014. `doi:10.1103/PhysRevSTAB.17.112001`

[7] S. Posen and D. L. Hall, "Nb_3Sn Superconducting Radiofrequency Cavities: Fabrication, Results, Properties, and Prospects," *Supercond. Sci. Techno.*, vol. 30, no. 3, p. 33004, Jan. 2017. `doi:10.1088/1361-6668/30/3/033004`

[8] D. L. Hall, M. Liepe, and J. T. Maniscalco, "RF Measurements on High Performance Nb_3Sn Cavities." presented at IPAC'17, Busan, Korea, May 2016, paper WEPMR024.

[9] M. Ge *et al.*, "CVD Coated Copper Substrate SRF Cavity Research at Cornell University," presented at SRF'19, Dresden, Germany, Jul. 2019, paper THFUA5.

[10] G. Gaitan *et al.*, "Development of a System for Coating SRF Cavities Using Remote Plasma CVD," presented at SRF'21, East Lansing, MI, USA, Jun. 2021, paper SUPTEV007, this conference.

[11] R. Valizadeh, "Synthesis of Nb and Alternative Superconducting Film to Nb for SRF Cavity as Single Layer," presented at SRF'21, East Lansing, MI, USA, Jun. 2021, paper FROFDV06, this conference.

[12] Z. Sun *et al.*, "Toward Stoichiometric and Low-Surface-Roughness Nb_3Sn Thin Films via Direct Electrochemical Deposition," presented at SRF'21, East Lansing, MI, USA, Jun. 2021, paper WEOTEV03, this conference.

[13] K. Howard, M. Liepe, and Z. Sun, "Thermal Annealing of Sputtered Nb_3Sn and V_3Si Thin Films for Superconducting RF Cavities," presented at SRF'21, East Lansing, MI, USA, Jun. 2021, paper SUPFDV009, this conference.

[14] Md. N. Sayeed *et al.*, "Cylindrical Magnetron Development for Nb_3Sn Deposition via Magnetron Sputtering," presented at SRF'21, East Lansing, MI, USA, Jun. 2021, paper THPTEV015, this conference.

[15] G. Rosaz *et al.*, "Development of Nb_3Sn Coatings by Magnetron Sputtering for SRF Cavities," presented at SRF'15, Whistler, BC, Canada, Sept. 2015, paper TUPB051

[16] N. Stilin, A. Holic, M. Liepe, R. Porter and J. Sears, "Stable CW Operation of Nb_3Sn SRF Cavity at 10 MV/m using Conduction Cooling," *arXiv preprint*, Feb. 2020, `arXiv:2002.11755v1`.

[17] G. Ciovati, G. Cheng, U. Pudasaini and R. A. Rimmer, "Multi-metallic conduction cooled superconducting radio-frequency cavity with high thermal stability," *Supercond. Sci. Techno.*, vol. 33, no. 7, May 2020. `doi:10.1088/1361-6668/ab8d98`

[18] R. C. Dhuley, S. Posen, M. I. Geelhoed, O. Prokofiev and J. C. T. Thangaraj, "First Demonstration of a Cryocooler Conduction Cooled Superconducting Radiofrequency Cavity Operating at Practical CW Accelerating Gradients," *Supercond. Sci. Techno.*, vol. 33, no. 6, Apr. 2020. `doi:10.1088/1361-6668/ab82f0`

[19] U. Pudasaini *et al.*, "Recent Results from Nb_3Sn Single Cell Cavities Coated at Jefferson Lab," presented at SRF'19, Dresden, Germany, Jul. 2019, paper MOP018.

[20] Z. Yang, Y. He, M. Lu and T. Tan, "Nb_3Sn Thin Film Cavity Development at IMP, CAS," presented at SRF'21, East Lansing, MI, USA, Jun. 2021, paper SUPFDV017, this conference.

[21] R. C. Dhuley *et al.*, "Advances in Nb_3Sn Superconducting Radiofrequency Cavities Towards First Practical Accelerator Applications," *Supercond. Sci. Techno.*, vol. 34, no. 2, Jan. 2021. `doi:10.1088/1361-6668/abc7f7`

[22] R. D. Porter *et al.*, "Field Limitation in Nb_3Sn Cavities," presented at SRF'19, Dresden, Germany, Jul. 2019, paper THFUA5, unpublished.

[23] R. D. Porter *et al.*, "Progress in Nb_3Sn SRF Cavities at Cornell University," in *Proc. NAPAC'19*, Lansing, MI, USA, Sep. 2019, paper MOYBB3.

[24] R. D. Porter, N. Banerjee, and M. Liepe "Dynamics of RF Dissipation Proved via High-Speed Temperature Mapping," presented at SRF'21, East Lansing, MI, USA, Jun. 2021, paper TUOFDV05, this conference.

[25] J. Vines, . Xie and H. Padamsee, "Systematic Trends for the Medium Field Q-Slope," presented at SRF'07, Beijing, China, Oct. 2007, paper TUP27.

[26] S. Aull, T. Junginger, H. Neupert and J. Knobloch, "Secondary Electron Yield of SRF Materials," presented at SRF'15, Whistler, BC, Canada, Sept. 2015, paper TUPB050.